Journal of Pathology
J Pathol 2013; **229:** 390–399
Published online 13 December 2012 in Wiley Online Library (wileyonlinelibrary.com) DOI: 10.1002/path.4074

ORIGINAL PAPER

Spontaneous and pronase-induced HER2 truncation increases the trastuzumab binding capacity of breast cancer tissues and cell lines

Daniele Recupero,[1] Lorenzo Daniele,[1] Caterina Marchiò,[1] Luca Molinaro,[1] Isabella Castellano,[1] Paola Cassoni,[1] Alberto Righi,[2] Filippo Montemurro,[3] Piero Sismondi,[4] Nicoletta Biglia,[4] Giuseppe Viale,[5] Mauro Risio[2] and Anna Sapino[1]*

[1] *Department of Biomedical Sciences and Human Oncology, University of Turin, via Santena 7 10126 Turin, Italy*
[2] *Department of Pathology, Institute for Cancer Research and Treatment (IRCC), Strada Provinciale 142, Km 3.95, 10060 Candiolo (Torino), Italy*
[3] *Division of Medical Oncology, Institute for Cancer Research and Treatment (IRCC), Strada Provinciale 142, Km 3.95, 10060 Candiolo (Torino), Italy*
[4] *Department of Gynaecological Oncology, University of Turin, Mauriziano Umberto I Hospital, Largo Filippo Turati, 62, 10128 Turin, Italy*
[5] *Department of Pathology, European Institute of Oncology, Via Ripamonti, 435, 20141 Milan, Italy*

**Correspondence to: Professor Anna Sapino, Department of Biomedical Sciences and Human Oncology, Via Santena 7, 10126 Turin, Italy. e-mail: anna.sapino@unito.it*

Abstract

A subgroup of HER2-overexpressing breast tumours co-expresses p95^{HER2}, a truncated HER2 receptor that retains a functional HER2 kinase domain but lacks the extracellular domain, thus impairing trastuzumab binding. We evaluated p95^{HER2} expression in 99 frozen breast carcinoma samples by western blot analysis. The HER2-positive cell line BT474 treated with pervanadate or pronase was used as a positive control for p95^{HER2} expression. Immunohistochemistry was performed on parallel formalin-fixed, paraffin-embedded sections of the same case series using antibodies directed against either the intra- or extra-cellular binding domain of HER2. In particular, biotinylated trastuzumab (BiotHER) was used to evaluate the binding capacity of the humanized antibody. To avoid a subjective evaluation of the score values and the percentage of immunostained cells, the slides were scanned and automatically analysed. The number of cases with HER2 overexpression (score 3+) and *HER2* gene amplification was higher in the p185^{HER2}-positive/p95^{HER2}-positive samples than in the p185^{HER2}-positive/p95^{HER2}-negative group. Automated analysis confirmed a significantly higher percentage of 3+ scored cells in p95^{HER2}-positive cases. Conversely, the percentage of 2+ scored cells was higher in p95^{HER2}-negative cases. The status of the HER2 extracellular domain was then studied using flow cytometry on BT474 cells after pronase enzymatic digestion using trastuzumab and pertuzumab, while the presence of HER2-HER3 dimers was studied using a proximity-ligation assay. *In vitro* experiments showed that short-term pronase digestion of BT474 cells produced two HER2 fragments (of 95 and 150 kDa, detectable in tissue specimens as well), increased the binding affinity of trastuzumab, reduced the rate of HER2–HER3 dimers, and did not interfere with pertuzumab-binding capacity. In conclusion, the presence of p95^{HER2} as detected by western blot analysis does not compromise the immunohistochemical detection of HER2. Our data suggest that a reduction of the receptor steric hindrance as induced by enzymatic shedding may facilitate the binding capacity of trastuzumab.

Keywords: breast cancer; HER2; p95^{HER2}; pronase; western blot; trastuzumab binding site

Received 27 March 2012; Revised 20 June 2012; Accepted 11 July 2012

No conflicts of interest were declared.

Introduction

The human proto-oncogene *HER2* encodes for the full-length membrane-spanning receptor p185^{HER2}. Over-expression of p185^{HER2} plays a pathogenic role in approximately 20% of breast cancers [1]. The large 110 kDa extracellular domain (ECD) of HER2 consists of 621 amino acids and is subdivided into four domains (I–IV) [2,3]. The HER2 ECD constitutively adopts an active extended conformation, which is acquired by other Epidermal Growth Factor Receptors (EGFRs) only after ligand binding. This structural feature of ECD favours the homo- and hetero-dimerization of HER2, thus encouraging activation of the intracellular tyrosine kinase domain and triggering downstream signalling events [4]. Pertuzumab, a humanized

monoclonal antibody, binds to HER2 near the centre of domain II and inhibits HER2 dimerization with other members of the EGFR family [5,6]. In contrast, binding of trastuzumab to domain IV of HER2 does not interfere with heregulin-induced HER2–HER3 dimer formation but prevents HER2 shedding and inhibits intracellular signalling [7].

Approximately 30% of HER2-positive patients express a variety of receptor fragments sized between 90 and 115 kDa. These are collectively known as $p95^{HER2}$ carboxy-terminal fragments (CTFs) [8]. In breast cancer, HER2-CTFs may be synthesized [9,10] or produced by an enzymatic sheddase [11]. A slow proteolytic cleavage performed by metalloproteases can occur at a site proximal to the transmembrane domain [12–14], thus generating a fragment of 95 kDa that retains kinase activity [15–19]. It is yet to be determined whether $p95^{HER2}$ levels in breast tumours are directly linked to the HER2 concentration in the serum [20–22]. The rapid and potent shedding of the HER2 ECD produced *in vitro* by pervanadate [23], a general inhibitor of protein-tyrosine phosphatases with a non-specific metalloprotease activation capacity, induces an increase in $p95^{HER2}$ levels in BT474 breast cancer cells and delivers the trastuzumab epitope to the cell culture medium [16]. Scaltriti *et al* [14] hypothesized that the tumours expressing $p95^{HER2}$ in the absence of the trastuzumab-binding extracellular domain may be resistant to the humanized antibody. However, a translational investigation from the neoadjuvant GeparQuattro study (incorporating chemotherapy plus trastuzumab treatment) showed that $p95^{HER2}$ expression, measured using a monoclonal antibody that specifically recognizes the 611 CTFs by immunohistochemistry (IHC), indicates a response to trastuzumab [24].

In previous studies using biotinylated trastuzumab (BiotHER) as the primary antibody for IHC [25,26], we demonstrated that the trastuzumab binding site was only detectable in approximately 50% of *HER2*-amplified breast cancers, while the reported percentage of HER2 overexpression using anti-intracellular domain (ICD) antibodies in amplified breast cancers is approximately 90% [27]. Similarly, we previously showed a lower percentage of ECD overexpression using the TAB250 antibody compared with the ICD expression as evaluated by CB11 in amplified breast cancers [28].

Taking these data together, our hypothesis was that the expression of HER2-truncated forms could reduce the availability of the epitopes necessary for a reaction with specific anti-ECD antibodies. Therefore, we evaluated the expression of the HER2-truncated forms by western blot (WB) analysis in a series of breast carcinomas and compared the level of expression with the IHC results using antibodies directed against both the ICD and the ECD of HER2. The results were compared and validated with those obtained *in vitro* in BT474 HER2-positive breast cancer cells after enzymatic induction of HER2 truncation.

Materials and methods

Tissue samples

Paired formalin-fixed, paraffin-embedded (FFPE) tissue blocks and snap-frozen specimens (stored at −80 °C in frozen tissue matrix OCT) from 99 breast cancers were obtained from the pathology files of the authors' institutions. The fixation was performed in buffered formalin at room temperature for 24–48 h. Permission for the project was obtained from the Institutional Review Board, and the study was conducted in compliance with the ethical regulatory requirements for the handling of biological specimens from tumour banks of the participating institutions (ie samples were exclusively available for research purposes in retrospective studies). The same Institutional Ethics Review Board agreed that written consent from the patients was not required, given that the study did not interfere with diagnosis or treatment decisions. The patient data were anonymized prior to analysis.

Fluorescence *in situ* hybridization (FISH)

FISH was performed using probes for *HER2* (17q12) and CEP17 (Vysis, Inc, Downers Grove, IL, USA) as previously reported [29]. The analysis was performed by selection and automated acquisition of six invasive areas on each slide using the Metafer Scanning System (Carl Zeiss MetaSystems GmbH, Baden-Wuttenberg, Germany) and AxioImager epifluorescence microscope. PathVysion V2 software (FDA approved) was used to analyse the results. The cases were scored according to the ASCO guidelines [30].

Immunostaining

The expression of the ICD was evaluated using the Herceptest™ kit (DAKO, Glostrup, Denmark) on a Dako Autostainer and CB11 (diluted 1 : 200; Novocastra Laboratories, Newcastle-upon-Tyne, UK) using a Bond™ automated stainer (Menarini Diagnostics, Florence, Italy). To evaluate the effect of $p95^{HER2}$ expression on ECD detection via IHC, the sections were processed using the TAB250 mouse monoclonal antibody (Zymed, San Francisco, CA, USA). In addition, to evaluate the trastuzumab-specific binding site, we used BiotHER as previously reported [25,26]. Briefly, 1 mg of trastuzumab was diluted in saline solution and dialysed overnight in 0.1 M Na_2CO_3, pH 8.5. To a 1 ml solution, 0.12 ml of aminohexanoyl-biotin-*N*-hydroxysuccinimide ester (AH-BNHS; Biospa, Milan, Italy) was added, gently mixed for 4 h at room temperature, and dialysed in phosphate buffered saline. We tested the ECD overexpression with or without pretreatment with pronase, diluted to 0.1%. Endogenous peroxidases were inhibited by incubating sections with 6% H_2O_2 for 7 min. The sections were then incubated with the primary antibodies diluted in PBS with 1% BSA (TAB250, 1 : 20; BiotHER, 1 : 100) for 30 min at room temperature. After rinsing in PBS, EnVision+

System Labelled Polymer-HRP (Dako) anti-mouse and HRP-conjugated streptavidin (diluted 1 : 50; BioGenex, San Ramon, CA, USA) were used to reveal TAB250 and BiotHER staining, respectively. The reaction was developed using a solution of 3,3′-diaminobenzidine and H_2O_2 for 5 min. The nuclei were counterstained with Mayer's haemalum.

To avoid a subjective evaluation of the percentage of immunostained cells in cancer tissues and to assess the intra-tumour heterogeneity of HER2 expression, BiotHER and CB11-stained slides were scanned and analysed using a ScanScope XT automated scanning system (Aperio Technologies, Vista, CA, USA) and the integrated FDA-approved software. Each section was subdivided into six quadrants in which eight to ten tumour foci were randomly selected (Figure 1). The score results (percentage of cells scored as 3+, 2+, and 1+) of each quadrant were recorded. A variance analysis comparing the percentage of positive cells in each quadrant was performed. The mean percentage of the different score values in each quadrant was then compared with the $p95^{HER2}$ status as defined by WB. Statistical analyses were performed using Student's *t*-test assuming unequal variances (software freely available at http://studentsttest.com/). The sections obtained from BT474 blocks (control and test) were processed with the same IHC protocols reported above.

In vitro induction of $p95^{HER2}$

To induce $p95^{HER2}$ production in BT474, cells were treated with freshly prepared pervanadate (0.5 M sodium orthovanadate and 0.5 M H_2O_2) [16]. After overnight starvation (DMEM with 0.5% FCS), the cells were treated with 0.1 or 1 mM pervanadate for 30, 60, 90, and 180 min. At each time point, the level of soluble $p97–115^{HER2}$ (the soluble circulating fragment of $p185^{HER2}$) was analysed in the supernatant using the human sHER2 enzyme-linked immunosorbent assay (ELISA) kit according to the manufacturer's instructions (BMS207; Bender MedSystems GmbH, Vienna, Austria). The results were normalized against non-conditioned medium. To test the effect on cell viability of H_2O_2 added to orthovanadate to obtain pervanadate, BT474 cells were incubated for 90 min either with 1 mM H_2O_2 alone or with the addition of 500 U/ml of catalase [31] after mixing orthovanadate and H_2O_2.

Alternatively, at confluence, BT474 cells were washed with PBS and treated with pronase (0.1% and 0.02% in PBS) at room temperature for 10 min. The cells were then collected and washed twice with PBS supplemented with 3× protease inhibitors cocktail (complete, EDTA-free; Roche Diagnostics SpA, Monza, Milan, Italy).

Cell growth was monitored in flasks with an EVOS inverted microscope (Advanced Microscopy Group, Bothell, WA, USA), and cell viability was assessed using trypan blue vital staining. Each experiment was performed in triplicate. The paraffin-embedded blocks were prepared from cell pellets obtained after fixation in buffered formalin.

Western blot (WB) analysis

After each treatment described above, the expression of HER2 was assessed by WB on BT474 cells. From the breast cancer specimens, ten frozen sections containing approximately 1 cm^2 of viable tumour cells were analysed. The adequacy was verified on haematoxylin and eosin-stained sections before and after cutting. One

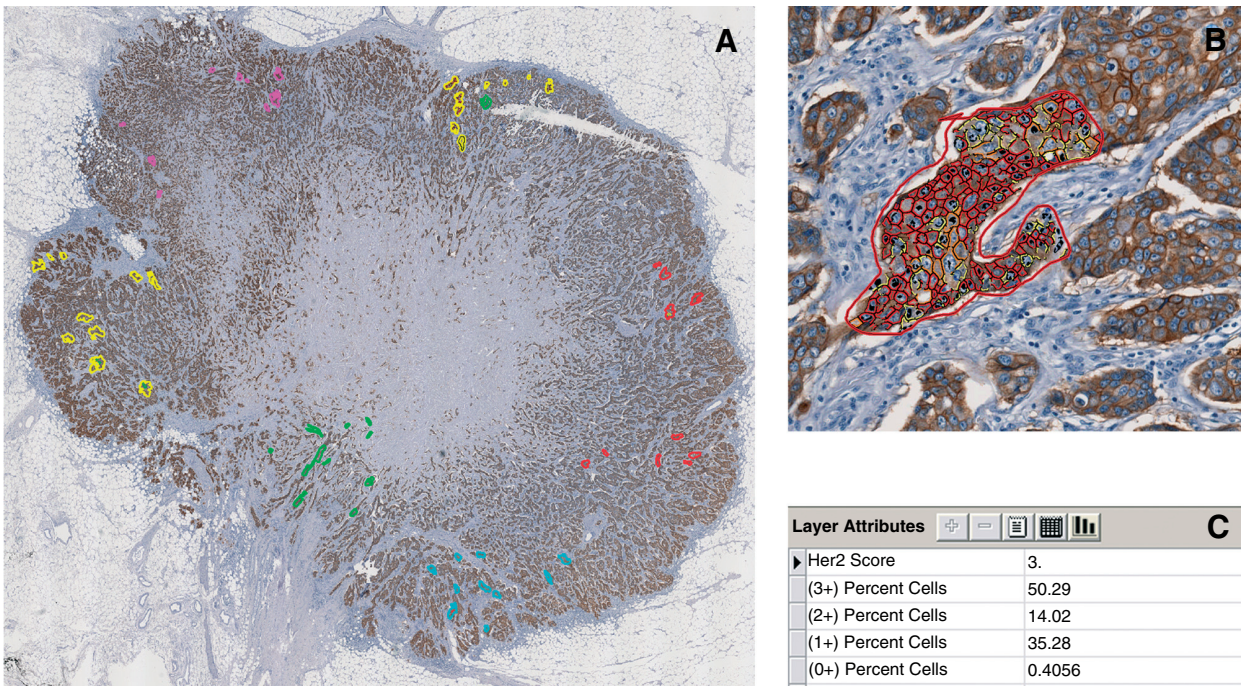

Figure 1. Automated IHC analysis. Micrographs illustrating an example of quadrant selection (A), the APERIO software result layout (B), and a table of the percentage of positivity (C).

out of 99 cases showing only *in situ* carcinoma on the frozen section was discarded. The frozen sections were collected in tubes and washed with cold PBS to remove the OCT and blood residues. The samples were lysed at 4 °C for 30 min in RIPA lysis buffer (50 mM Tris–HCl, pH 7.5; 150 mM NaCl; 1% Triton X-100; and 0.1% SDS) with protease inhibitors. The total protein extracts were quantified with the BCA protein assay (Thermo Fisher Scientific Inc, Rockford, IL, USA), divided into aliquots of 25 µg, and stored at −80 °C.

After the addition of 5× loading buffer, each sample was boiled for 5 min and loaded onto an 8% polyacrylamide gel. Each gel contained a control lane loaded with 25 µg of protein extracted from pervanadate-treated BT474 cells as a marker for $p95^{HER2}$.

Electrophoresis was performed in TGS buffer; after separation, proteins were transferred to a nitrocellulose membrane. After saturation with TBS and 5% milk, the membrane was immunoblotted either with anti-HER2 (A0485, polyclonal antibody; Dako, Glostrup, Denmark) at 1 : 1000 or with anti-actin at 1 : 800 as a loading control. Both antibodies were diluted in TBS with 5% BSA and incubated overnight at 4 °C. The membrane was washed and incubated with an anti-rabbit peroxidase-labelled secondary antibody. Finally, the membrane was developed with ECL luminol (Bio-Rad, Hercules, CA, USA).

$p185^{HER2}$ was considered overexpressed (++) if the WB band was greater than or equal to the $p185^{HER2}$ level in 25 µg of BT474 cells. Lower $p185^{HER2}$ expression levels were classified as $p185^{HER2}$ (+). Specimens were scored as positive for $p95^{HER2}$ (+) if a distinct band was present at the same molecular weight as the $p95^{HER2}$ pervanadate-induced band in BT474 cell extracts.

Flow cytometry

To obtain a single cell suspension, BT474 cells were detached with trypsin/EDTA and collected into a 50 ml tube with 20 ml of DMEM medium at 37 °C for 1 h to allow the replacement of all the surface molecules eventually digested by trypsin. Afterwards, four tubes of 10^6 cells each were centrifuged. Two cell pellets were incubated for 10 min at room temperature with 100 µl of 0.1% pronase; controls were kept in PBS. To ensure complete pronase inactivation, the cells were washed once with DMEM and twice with PBS supplemented with 2× protease inhibitors. The cells were then incubated at room temperature for 30 min with trastuzumab or pertuzumab (Genentech, Inc, South San Francisco, CA, USA), both at a final concentration of 100 ng/ml, followed by a FITC-conjugated anti-human secondary antibody. The stained cells were analysed with a Canto II flow cytometer (Becton Dickinson, San Jose, CA, USA).

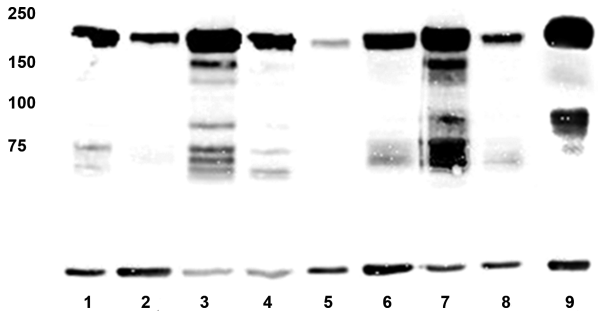

Figure 2. Western blot analysis performed on breast cancer tissues. $p185^{HER2}$++/$p95^{HER2}$−cases (lanes 1, 2, 4, and 6), $p185^{HER2}$++/$p95^{HER2}$+ cases (lanes 3 and 7), $p185^{HER2}$+/$p95^{HER2}$−cases (lanes 5, and 8), and pervanadate-treated BT474 cells (lane 9). A subgroup of cases with high expression of $p185^{HER2}$ and $p95^{HER2}$ showed a 150 kDa fragment (lanes 3 and 7).

Immunoprecipitation analyses

The pronase-treated BT474 cells were lysed in RIPA buffer as described above. Total extract aliquots of 500 µg were incubated with 2 µg of trastuzumab or pertuzumab at 4 °C overnight under gentle agitation. Twenty microlitres of sepharose-protein A and sepharose-protein G beads was added. After incubation for 2 h at 4 °C, the sepharose beads were washed and rinsed with 1× loading buffer. The immunoprecipitated proteins and 25 µg of control total extracts were analysed by western blot using the same protocol described above.

Proximity ligation assay (PLA)

All reagents used for the PLA analysis were from Olink Bioscience (Uppsala Science Park, Uppsala, Sweden). The PLA reactions were performed following the manufacturer's instructions using anti-HER2 (A0485 polyclonal diluted 1 : 300) and anti-HER3 (monoclonal antibody clone 6F12 diluted 1 : 100; Lab Vision, Thermo Fisher Scientific Inc, Kalamazoo, MI, USA) as primary antibodies. Student's *t*-test was used assuming unequal variances.

Results

Correlation of $p95^{HER2}$ and IHC results in breast cancer specimens

By WB analysis, $p185^{HER2}$ was detectable in 50 cases. Forty samples showed *HER2* amplification by FISH. Among these amplified cases, 20 were $p185^{HER2}$++, and 12 of these also expressed $p95^{HER2}$ by WB (Figure 2). In the latter subgroup of cases, five showed a 150 kDa fragment as well. Twenty cases $p185^{HER2}$+ were negative for $p95^{HER2}$. Two out of seven cases with *HER2* gene gain (less than six gene signals per cell) had high expression levels of $p185^{HER2}$, but not $p95^{HER2}$. Three cases with very low expression levels of $p185^{HER2}$ did not show any genetic alterations.

Table 1. Correlation of $p185^{HER2}$ and $p95^{HER2}$ expression by western blot and score 3+ immunohistochemical results (>10% of HER2-positive cells with strong and complete membrane expression) with anti-HER2 antibodies in 50 breast cancers

	Immunohistochemistry score 3+ of HER2			
	Anti-intracellular domain		Anti-extracellular domain	
Western blot	CB11 (%)	A048 (%)	TAB250 (%)	BiotHER (%)
p185++/p95+	9/12 (75)	7/12 (58)	8/12 (67)	7/12 (58)
p185++/p95−	3/10 (30)	4/10 (40)	4/10 (40)	4/10 (40)

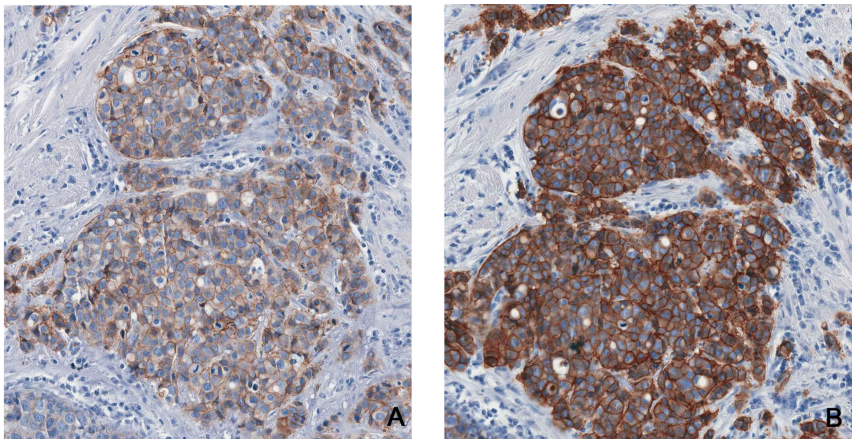

Figure 3. Pronase antigen retrieval. A breast carcinoma sample immunostained with BiotHER following routine IHC procedure (no antigen retrieval) (A). Pronase antigen retrieval increases both the percentage and the intensity of immunostaining (B).

The effect of $p95^{HER2}$ expression on the HER2 IHC expression of breast cancer tissues is shown in Table 1. The number of cases showing HER2 overexpression (score 3+; >10% of HER2+ cells with strong and complete membrane staining) was higher in the series scored as $p185^{HER2}$++/$p95^{HER2}$+ by WB than in the series $p185^{HER2}$++/$p95^{HER2}$−. This result was confirmed using both the anti-ICD (Herceptest™ and CB11) and the anti-ECD (TAB250 and BiotHER) antibodies following antigen retrieval with pronase. Pronase increased the 3+ scored cells with BiotHER and TAB250 (Figure 3) antibodies compared with sections not enzyme treated, regardless of the level of $p95^{HER2}$.

Automated analysis of CB11 and BiotHER immunostaining of breast cancer confirmed a significantly higher percentage of 3+ scored cells in $p95^{HER2}$+ cases compared with the $p95^{HER2}$− ($p < 0.005$; Figures 4A and 4D). In contrast, the percentage of 2+ scored cells was higher in $p95^{HER2}$− cases ($p < 0.005$; Figures 4B and 4E). In both series, the immunostaining was homogeneously distributed. The percentage of cells scored 1+ was similar in the two groups ($p > 0.005$; Figures 4C and 4F). No significant differences among the 3+ ($p >> 0.005$), 2+ ($p >> 0.005$), and 1+ ($p >> 0.005$) quadrants were observed at variance analysis, indicating uniform quadrant selection.

$p95^{HER2}$ induction and cell viability in BT474

Incubation of BT474 cells with pervanadate (1 mM) induced a shedding of HER2 ECD that increased in a time-dependent manner, as shown by the ELISA test (Figure 5A); this occurred in parallel to the $p95^{HER2}$ increase (Figure 5B). However, BT474 cells rapidly detached from the culture plate, and cell viability was highly compromised by the treatment with pervanadate even after 30 min of exposure (Figures 6A and 6B), with almost 80% cell death. The toxic effect of pervanadate was confirmed when catalase was used to block excess H_2O_2 (Figure 6C). In contrast, H_2O_2 alone did not induce any sign of cellular stress (Figure 6D). Lower concentrations of pervanadate (0.1 mM) did not induce $p95^{HER2}$ even after 3 h of treatment (Figure 5C) but maintained the cytotoxic effect.

Pronase treatment digested $p185^{HER2}$ and generated two fragments (Figure 7), and did not compromise cell viability, as shown by EVOS examination (Figures 6E and 6F) and trypan blue assay. The cells treated with 0.02% pronase showed a thin $p95^{HER2}$ band, a clear and intense band at 150 kDa, and maintained strong expression of $p185^{HER2}$. Higher pronase concentrations (0.1%) led to a further increase in the 95 kDa and 150 kDa band signals coupled with an almost complete disappearance of the p185 band (Figure 7).

Trastuzumab and pertuzumab binding

Membrane immunostaining with BiotHER following pronase treatment increased in intensity (Figure 8). Flow cytometry on control BT474 cells showed 67% of cells with higher trastuzumab affinity and the remaining 33% with lower affinity for trastuzumab (Figure 9A). After 10 min of pronase exposition, 94%

3+	p95+	p95-
M q1	40,73	16,15
M q2	36,4	20,77
M q3	44,78	19,33
M q4	43,28	23,2
M q5	34,18	27,29
M q6	44,5	35,25

2+	p95+	p95-
M q1	17,82	34,77
M q2	19,1	32,77
M q3	16	32,08
M q4	14,56	32,5
M q5	18,78	27,86
M q6	18	27,25

1+	p95+	p95-
M q1	37,5	41,92
M q2	38,86	39,92
M q3	32,67	39,18
M q4	35,67	37
M q5	40,17	34
M q6	36,5	34,75

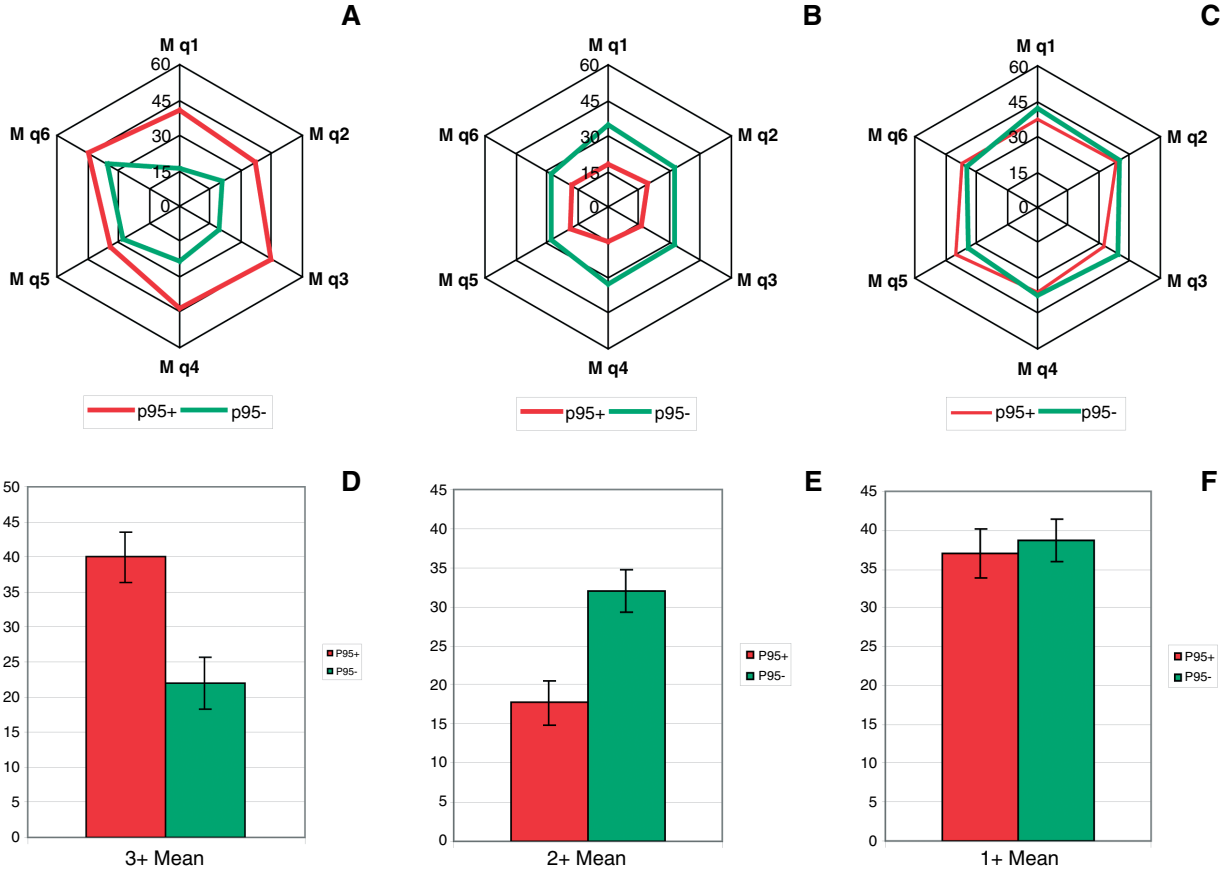

Figure 4. Automated analysis of HER2 extracellular domain expression by IHC. Distribution of the mean percentage of BiotHER expression within six different fields (ie section quadrants Mq_{1-6}) (A–C). Differences between $p95^{HER2}$-positive (red) and -negative (green) cases are statistically significant in 3+ score (A, D) and 2+ score (B, E) categories, whereas no statistically significant difference is observed in 1+ scored cases (C, F).

of cells showed high trastuzumab binding (Figure 9B). By immunoprecipitation, we showed that the 150 kDa HER2 fragment induced by pronase treatement still bound trastuzumab (Figure 10). Pronase treatment did not affect the binding capacity of pertuzumab, as shown by flow cytometry (Figures 9C and 9D) and confirmed by immunoprecipitation assay (Figure 10).

HER2–HER3 dimer dissociation

The PLA performed using anti-HER2 and -HER3 antibodies allowed for the analysis of heterodimers in BT474. The mean number of signals per cell (mean = 20.30; mode = 18; standard deviation = 10.53; $n = 315$) in the control was significantly higher ($p < 0.005$), as determined by a t-test analysis, than the mean number of signals per cell (mean = 13.76; mode = 5; standard deviation = 9.88; $n = 384$) in the BT474 pronase-treated cells (Figure 11).

Discussion

Our first objective was to evaluate whether $p95^{HER2}$ may impair the trastuzumab-binding epitope. Using WB and IHC analyses, we confirmed the results by Molina *et al* [18] demonstrating that $p95^{HER2}$ fragments in breast cancer tissues are generally associated with high levels of $p185^{HER2}$. However, in contrast to our expectations, we observed that the IHC expression of the trastuzumab epitope as detected by BiotHER in breast cancer tissue was higher in $p95^{HER2}$+ cases than

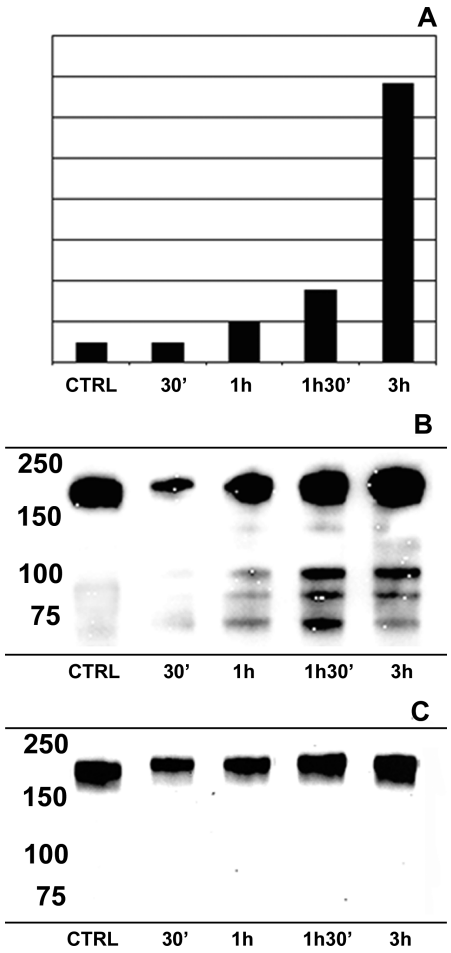

Figure 5. Induction of HER2 shedding on BT474 cells by pervanadate. HER2 ECD levels in culture medium as evaluated by ELISA increase after 1 mM pervanadate treatment (A), which in parallel induce $p95^{HER2}$ as shown by western blot (B). No $p95^{HER2}$ induction was observed using 0.1 mM pervanadate (C).

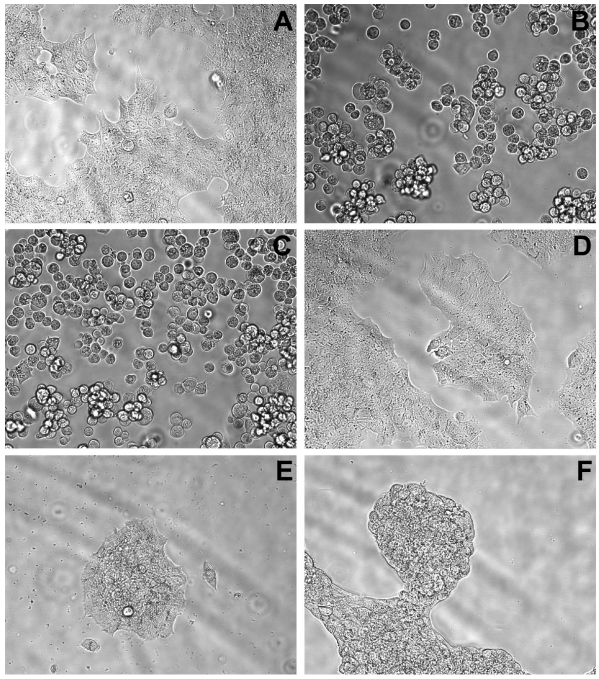

Figure 6. Effects of proteolytic treatments on cell cultures. Control BT474 cells (A, E). Following 1 mM pervanadate alone (B) or pervanadate and catalase treatment (C), BT474 cells detach from the dish and die (B). Cell viability is not compromised in BT474 cells treated with 1 mM hydrogen peroxide alone (D) and in BT474 cells treated with 0.1% pronase (F).

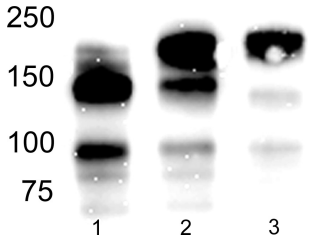

Figure 7. Pronase induced HER2 cleavage. Treatment with 0.1% pronase (lane 1) and 0.02% pronase (lane 2) in BT474 cells leads to $p185^{HER2}$ cleavage and the formation of 150 kDa and 95 kDa bands. Control BT474 cells (lane 3).

in cases with similar high levels of $p185^{HER2}$ but negative for $p95^{HER2}$. This result could explain the response of tumours that expressed $p95^{HER2}$ to trastuzumab therapy measured by IHC as shown in the neoadjuvant GeparQuattro study [24].

A possible explanation for this unexpected increase in immunoreactivity of the anti-HER2 antibodies in the presence of truncated HER2 may be the reduction of the antigen 'steric hindrance'. It has been demonstrated that the number of antigen molecules that are bound to the cell surface could significantly affect the ability of antibodies to bind, causing steric hindrance [32]. If the antigenic determinants are closely spaced on the cell surface, spatial interference may result such that a smaller distance between the antigenic determinants leads to a greater likelihood of reduced antibody binding. In previous experiments, Valabrega *et al* [33] were able to modulate the expression of HER2 in SKBR3 HER2-overexpressing breast cancer cells by using small interfering RNAs at different concentrations. In agreement with our hypothesis, it was shown that a HER2 reduction up to 70%, as measured by WB analysis and flow cytometry, still corresponded to an immunoreactivity of cells scored as 3+ and that HER2 reduction up to 40% rendered cancer cells more sensitive to trastuzumab treatment.

To study the effect of HER2 truncation *in vitro*, as suggested by others [16], we used pervanadate, a protein-tyrosine phosphatase inhibitor that induces HER2 shedding in BT474 cells through non-specific metalloprotease activity. Unfortunately, we found pervanadate to be highly toxic. An alternative method to test our hypothesis was to simulate proteolysis by treating cells directly with a cocktail of proteases known as pronase, a mixture of at least ten proteases [34] commonly used in IHC for antigen retrieval of FFPE tissues. Digestion using pronase-based solutions is designed to break the protein cross-links and unmask the antigens and epitopes in FFPE tissue sections, enhancing the antibody staining intensity [35]. In addition, pronase treatment of high-molecular-weight

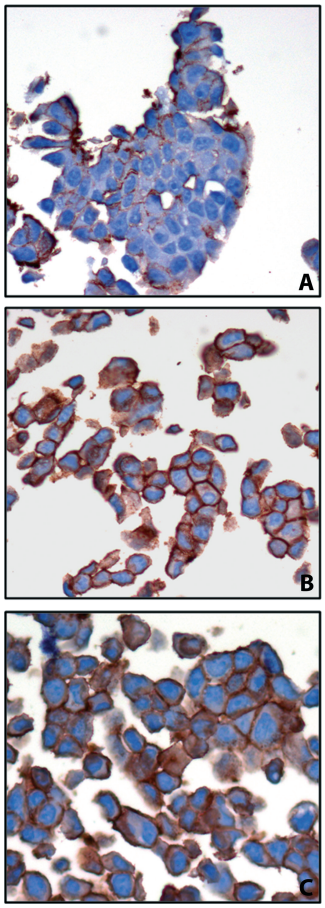

Figure 8. Effects of proteolytic treatments on the expression of trastuzumab binding site in BT474 cells. BiotHER staining in control BT474 cells (A), *in vitro* pronase-treated cells (B), or pronase antigen retrieval of sections cut from FFPE cell blocks (C). Stronger and more diffuse staining is observed in BT474 cells treated with pronase (B) and in sections following pronase antigen retrieval (C).

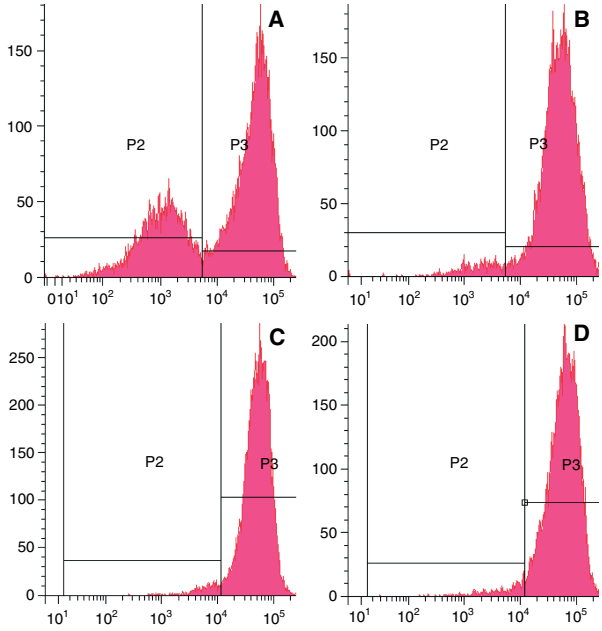

Figure 9. Flow cytometry analysis on BT474 cells. Flow cytometry analysis on control BT474 cells shows two populations, one (67% of cells) with high trastuzumab affinity compared with the remaining 33% with lower affinity (A). After 10 min of pronase exposition, there is a shift to 94% of cells with high affinity (B). The binding capacity of pertuzumab is not affected by pronase treatment (C, D).

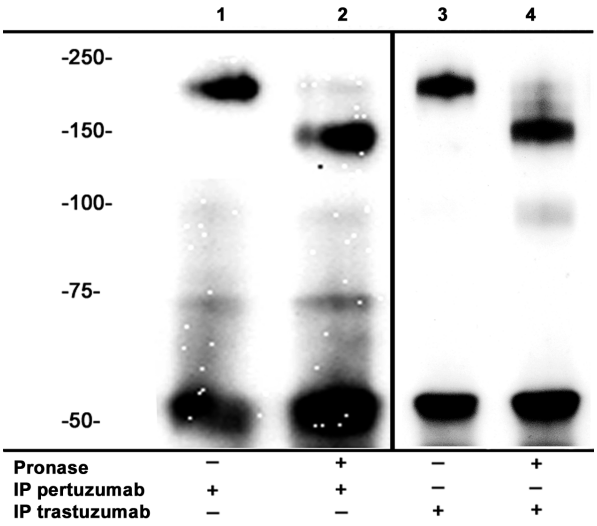

Figure 10. Pertuzumab and trastuzumab binding site. Immunoprecipitated HER2 protein using pertuzumab or trastuzumab shows a band at 180 kDa in control (lanes 1 and 3) and at 150 kDa in pronase-treated (lanes 2 and 4) BT474 cells, confirming the presence of the antibody binding site.

glycoproteins is a useful method for obtaining glycoprotein fragmentation without significant loss of biological activity [36]. We demonstrated that pronase treatment of BT474 cells led to a proteolytic cleavage of HER2 with the formation of 95 kDa and 150 kDa fragments without affecting cell viability. In turn, this proteolysis increased trastuzumab affinity, did not affect pertuzumab-binding capacity, and reduced HER2–HER3 dimer formation in breast cancer cells. The principal explanation for the triple effect of pronase could be the unmasking of the trastuzumab antigenic epitope and the shedding of domain I that leads to the formation of the 150 kDa fragment. This HER2 fragment is likely to maintain the integrity of the pertuzumab-binding domains, while the blocking of the interaction of domain I with domain III may inhibit the open conformation of HER2 and prevent dimer formation [5,37–39]. By WB, we showed that the 150 kDa fragment is present in human breast cancer tissues as well.

The size of the antibody molecule (150 kDa for IgG) may be another source of interference, particularly if the epitopes are closely spaced. Thus, steric hindrance is likely to be intensified when the antibodies have been labelled with other molecules such as biotin. In our IHC tissue protocol, the effect of trastuzumab biotinylation on the avidin–biotin reaction was controlled by using aminocaproate, which limits the steric hindrance by providing a six-carbon spacer to biotin and thus improves accessibility to the binding site on avidin.

In conclusion, we have shown that the presence of $p95^{HER2}$ increases the trastuzumab-binding capacity in cancer tissues. The shedding phenomenon induced

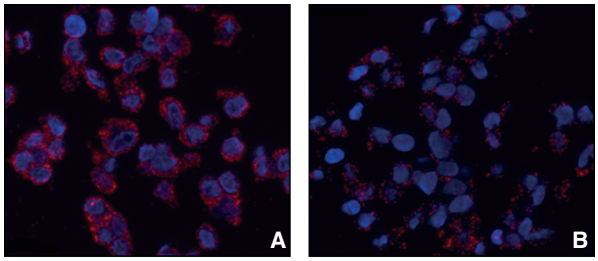

Figure 11. PLA analysis on HER2/HER3 dimer. Dimers are identified by the fluorescent signals (red spots): a higher number of dimers is observed in control BT474 cells (A) than in pronase-treated BT474 cells (B).

in vivo by metalloprotease and *in vitro* by pronase could thus improve the binding of antibodies with specific HER2 epitopes and allow trastuzumab to more efficiently reach its epitope by reducing the steric hindrance of cancer cells that may carry millions of $p185^{HER2}$ molecules on their surface.

Acknowledgment

We thank Dr Alessandra Stacchini for support with flow cytometry experiments. This study was funded by Ricerca Sanitaria Finalizzata Regione Piemonte 2009, Rete Oncologica Piemonte e Valle d'Aosta 2010, Ricerca Sanitaria Finalizzata RF-2010-2310674 and AIRC Grants (IG 10787 to AS and MFAG 13310 to CM).

Author contribution statement

DR performed all the experiments, participated in the coordination of the study, and helped draft the manuscript. LD performed the statistical analysis. CM participated in the case collection, in FISH analysis, and in revision of the manuscript. LM performed the slides' scanning and analyses of the virtual slides. IC and PC revised the immunohistochemical data. AR participated in the case collection and revision of the immunohistochemical data. FM participated in the writing of the manuscript. PS and NB performed surgery and provided surgical specimens. GV and MR contributed to case series and histopathological revision. AS conceived and designed the study, analysed the data, and wrote the final manuscript.

References

1. Slamon DJ, Clark GM, Wong SG, *et al*. Human breast cancer: correlation of relapse and survival with amplification of the HER-2/neu oncogene. *Science* 1987; **235**: 177–182.
2. Cho HS, Mason K, Ramyar KX, *et al*. Structure of the extracellular region of HER2 alone and in complex with the Herceptin Fab. *Nature* 2003; **421**: 756–760.
3. Pal SK, Pegram M. Targeting HER2 epitopes. *Semin Oncol* 2006; **33**: 386–391.
4. Moasser MM. The oncogene HER2: its signaling and transforming functions and its role in human cancer pathogenesis. *Oncogene* 2007; **26**: 6469–6487.
5. Franklin MC, Carey KD, Vajdos FF, *et al*. Insights into ErbB signaling from the structure of the ErbB2–pertuzumab complex. *Cancer Cell* 2004; **5**: 317–328.
6. Adams CW, Allison DE, Flagella K, *et al*. Humanization of a recombinant monoclonal antibody to produce a therapeutic HER dimerization inhibitor, pertuzumab. *Cancer Immunol Immunother* 2006; **55**: 717–727.
7. Badache A, Hynes NE. A new therapeutic antibody masks ErbB2 to its partners. *Cancer Cell* 2004; **5**: 299–301.
8. Parra-Palau JL, Pedersen K, Peg V, *et al*. A major role of p95/611-CTF, a carboxy-terminal fragment of HER2, in the down-modulation of the estrogen receptor in HER2-positive breast cancers. *Cancer Res* 2010; **70**: 8537–8546.
9. Anido J, Scaltriti M, Bech Serra JJ, *et al*. Biosynthesis of tumorigenic HER2 C-terminal fragments by alternative initiation of translation. *EMBO J* 2006; **25**: 3234–3244.
10. Pedersen K, Angelini PD, Laos S, *et al*. A naturally occurring HER2 carboxy-terminal fragment promotes mammary tumor growth and metastasis. *Mol Cell Biol* 2009; **29**: 3319–3331.
11. Yuan CX, Lasut AL, Wynn R, *et al*. Purification of Her-2 extracellular domain and identification of its cleavage site. *Protein Expr Purif* 2003; **29**: 217–222.
12. Carney WP, Neumann R, Lipton A, *et al*. Potential clinical utility of serum HER-2/neu oncoprotein concentrations in patients with breast cancer. *Clin Chem* 2003; **49**: 1579–1598.
13. Sanderson MP, Dempsey PJ, Dunbar AJ. Control of ErbB signaling through metalloprotease mediated ectodomain shedding of EGF-like factors. *Growth Factors* 2006; **24**: 121–136.
14. Scaltriti M, Rojo F, Ocana A, *et al*. Expression of p95HER2, a truncated form of the HER2 receptor, and response to anti-HER2 therapies in breast cancer. *J Natl Cancer Inst* 2007; **99**: 628–638.
15. Christianson TA, Doherty JK, Lin YJ, *et al*. NH2-terminally truncated HER-2/neu protein: relationship with shedding of the extracellular domain and with prognostic factors in breast cancer. *Cancer Res* 1998; **58**: 5123–5129.
16. Codony-Servat J, Albanell J, Lopez-Talavera JC, *et al*. Cleavage of the HER2 ectodomain is a pervanadate-activable process that is inhibited by the tissue inhibitor of metalloproteases-1 in breast cancer cells. *Cancer Res* 1999; **59**: 1196–1201.
17. Molina MA, Codony-Servat J, Albanell J, *et al*. Trastuzumab (herceptin), a humanized anti-Her2 receptor monoclonal antibody, inhibits basal and activated Her2 ectodomain cleavage in breast cancer cells. *Cancer Res* 2001; **61**: 4744–4749.
18. Molina MA, Saez R, Ramsey EE, *et al*. NH(2)-terminal truncated HER-2 protein but not full-length receptor is associated with nodal metastasis in human breast cancer. *Clin Cancer Res* 2002; **8**: 347–353.
19. Saez R, Molina MA, Ramsey EE, *et al*. p95HER-2 predicts worse outcome in patients with HER-2-positive breast cancer. *Clin Cancer Res* 2006; **12**: 424–431.

20. Leitzel K, Teramoto Y, Konrad K, *et al*. Elevated serum c-erbB-2 antigen levels and decreased response to hormone therapy of breast cancer. *J Clin Oncol* 1995; **13**: 1129–1135.
21. Tsé C, Gauchez AS, Jacot W, *et al*. HER2 shedding and serum HER2 extracellular domain: biology and clinical utility in breast cancer. *Cancer Treat Rev* 2012; **38**: 133–142.
22. Yamauchi H, O'Neill A, Gelman R, *et al*. Prediction of response to antiestrogen therapy in advanced breast cancer patients by pretreatment circulating levels of extracellular domain of the HER-2/c-neu protein. *J Clin Oncol* 1997; **15**: 2518–2525.
23. Tsiani E, Fantus IG. Vanadium compounds biological actions and potential as pharmacological agents. *Trends Endocrinol Metab* 1997; **8**: 51–58.
24. Loibl S, Bruey J, Von Minckwitz G, *et al*. Validation of p95 as a predictive marker for trastuzumab-based therapy in primary HER2-positive breast cancer: a translational investigation from the neoadjuvant GeparQuattro study. *J Clin Oncol* 2011; **29**: 2011 (suppl; abstr 530).
25. Bussolati G, Montemurro F, Righi L, *et al*. A modified trastuzumab antibody for the immunohistochemical detection of HER-2 overexpression in breast cancer. *Br J Cancer* 2005; **92**: 1261–1267.
26. Sapino A, Montemurro F, Marchio C, *et al*. Patients with advanced stage breast carcinoma immunoreactive to biotinylated Herceptin are most likely to benefit from trastuzumab-based therapy: an hypothesis-generating study. *Ann Oncol* 2007; **18**: 1963–1968.
27. Sapino A, Marchio C, Senetta R, *et al*. Routine assessment of prognostic factors in breast cancer using a multicore tissue microarray procedure. *Virchows Arch* 2006; **449**: 288–296.
28. Sapino A, Coccorullo Z, Cassoni P, *et al*. Which breast carcinomas need HER-2/neu gene study after immunohistochemical analysis? Results of combined use of antibodies against different c-erbB2 protein domains. *Histopathology* 2003; **43**: 354–362.
29. Marchio C, Lambros MB, Gugliotta P, *et al*. Does chromosome 17 centromere copy number predict polysomy in breast cancer? A fluorescence *in situ* hybridization and microarray-based CGH analysis. *J Pathol* 2009; **219**: 16–24.
30. Wolff AC, Hammond ME, Schwartz JN, *et al*. American Society of Clinical Oncology/College of American Pathologists guideline recommendations for human epidermal growth factor receptor 2 testing in breast cancer. *J Clin Oncol* 2007; **25**: 118–145.
31. Thoroed SM, Bryan-Sisneros A, Doroshenko P. Protein phosphotyrosine phosphatase inhibitors suppress regulatory volume decrease and the volume-sensitive Cl-conductance in mouse fibroblasts. *Pflugers Arch* 1999; **438**: 133–140.
32. Kent SP, Ryan KH, Siegel AL. Steric hindrance as a factor in the reaction of labeled antibody with cell surface antigenic determinants. *J Histochem Cytochem* 1978; **26**: 618–621.
33. Valabrega G, Giordano S, Montemurro F, *et al*. Non-linear relationship between HER2 expression and response to trastuzumab in breast cancer. *Ann Oncol* 2006; **17**: xi9.
34. Jurasek J, Johnson P, Olafson RW, *et al*. An improved fractionation system for pronase on CM-sephadex. *Can J Biochem* 1971; **49**: 1195–1201.
35. Shi SR, Chaiwun B, Young L, *et al*. Antigen retrieval technique utilizing citrate buffer or urea solution for immunohistochemical demonstration of androgen receptor in formalin-fixed paraffin sections. *J Histochem Cytochem* 1993; **41**: 1599–1604.
36. Watanabe K, Tsuge Y, Shimoyamada M, *et al*. Antitumor effects of pronase-treated fragments, glycopeptides, from ovomucin in hen egg white in a double grafted tumor system. *J Agric Food Chem* 1998; **46**: 3033–3038.
37. Dawson JP, Bu Z, Lemmon MA. Ligand-induced structural transitions in ErbB receptor extracellular domains. *Structure* 2007; **15**: 942–954.
38. Burgess AW, Cho HS, Eigenbrot C, *et al*. An open-and-shut case? Recent insights into the activation of EGF/ErbB receptors. *Mol Cell* 2003; **12**: 541–552.
39. Schlessinger J. Ligand-induced, receptor-mediated dimerization and activation of EGF receptor. *Cell* 2002; **110**: 669–672.